JCI insight

RESEARCH ARTICLE

Flow virometric sorting and analysis of HIV quasispecies from plasma

Thomas Musich,[1] Jennifer C. Jones,[2] Brandon F. Keele,[3] Lisa M. Miller Jenkins,[4] Thorsten Demberg,[1] Thomas S. Uldrick,[5] Robert Yarchoan,[5] and Marjorie Robert-Guroff[1]

[1]Immune Biology of Retroviral Infection Section and [2]Molecular Immunogenetics and Vaccine Research Section, Vaccine Branch, National Cancer Institute, Bethesda, Maryland, USA. [3]AIDS and Cancer Virus Program, Leidos Biomedical Research Inc., Frederick National Laboratory for Cancer Research, Frederick, Maryland, USA. [4]Collaborative Protein Technology Resource, Laboratory of Cell Biology, National Cancer Institute, Bethesda, Maryland, USA. [5]Retroviral Diseases Section, HIV and AIDS Malignancy Branch, National Cancer Institute, Bethesda, Maryland, USA.

Flow cytometry is utilized extensively for cellular analysis, but technical limitations have prevented its routine application for characterizing virus. The recent introduction of nanoscale fluorescence-activated cytometric cell sorting now allows analysis of individual virions. Here, we demonstrate staining and sorting of infectious HIV. Fluorescent antibodies specific for cellular molecules found on budding virions were used to label CCR5-tropic Bal HIV and CXCR4-tropic NL4.3 HIV Env-expressing pseudovirions made in THP-1 cells (monocyte/macrophage) and H9 cells (T cells), respectively. Using a flow cytometer, we resolved the stained virus beyond isotype staining and demonstrated purity and infectivity of sorted virus populations on cells with the appropriate coreceptors. We subsequently sorted infectious simian/human immunodeficiency virus from archived plasma. Recovery was approximately 0.5%, but virus present in plasma was already bound to viral-specific IgG generated in vivo, likely contributing to the low yield. Importantly, using two broadly neutralizing HIV antibodies, PG9 and VRC01, we also sorted virus from archived human plasma and analyzed the sorted populations genetically and by proteomics, identifying the quasispecies present. The ability to sort infectious HIV from clinically relevant samples provides material for detailed molecular, genetic, and proteomic analyses applicable to future design of vaccine antigens and potential development of personalized treatment regimens.

Introduction

Virology as a scientific discipline has always been hampered by technological limitations associated with analyzing submicron particles, particularly in a high-throughput setting. Flow cytometry has the potential to contribute to the field of virology as a whole, and to HIV research in particular, by overcoming these limitations. Methods for utilizing flow cytometry on individual virions are just now being developed. Early attempts were made to examine T2 phage and reovirus particles by flow cytometry, utilizing a custom flow cytometer to resolve virions by light scattering alone (1). The results indicated a need for further refinement, such as augmenting light scattering by fluorescent staining of viral nucleic acid, protein, or lipid components, in order to resolve virions of similar size and/or shape. Various strategies have sought to utilize nucleic acid fluorescent labeling to detect virions, but this has proven problematic, as this label is interior to the viral membrane and may require staining methods that interfere with the infectivity of the virus. Using SYBR green fluorescence for staining nucleic acid, viruses from several families were detected using a standard flow cytometer; however, viruses similar in size to HIV remained below the detectable limit (2). This staining protocol also required fixation, which would affect viral infectivity following cytometric analysis. Nucleic acid fluorescence has since been utilized effectively to purify intracellular herpes virus intermediates (3), but nucleic acid fluorescence is difficult to apply to a virus like HIV, especially if one wishes to detect and sort it from biologic samples such as patient plasma.

For biologically relevant particles or viruses with diameters of around 100 nm, such as HIV, distinction from background is a significant issue impeding accurate detection by conventional flow cytometry (4). Care is needed to ensure individual particle detection rather than swarm detection (5). An additional consideration is the utilization of the correct trigger channel threshold in order to properly detect virus

Conflict of interest: The authors have declared that no conflict of interest exists.

Submitted: September 14, 2016
Accepted: January 5, 2017
Published: February 23, 2017

Reference information:
JCI Insight. 2017;2(4):e90626. https://doi.org/10.1172/jci.insight.90626.

over background noise (6). Put simply, if the proper controls are not in place for small particles, incorrect conclusions can result from flow cytometry data. The technical considerations that must be applied to effectively utilize flow cytometry for analysis of HIV virions are numerous, but the potential for significant contributions to the field of virology is substantial.

Recently, new applications of flow cytometry techniques have led to new methods of virological analysis. Using magnetic nanoparticles bound to antibodies specific for viral proteins, HIV-1 virions were analyzed by flow cytometry without the limitation of the small size of the virus (7). Similar techniques were subsequently applied to Dengue virus (8). Individual virions have been analyzed directly by flow cytometric methods, specifically Nipah virus–like particles after labeling with glycoprotein-specific antibodies (9) and CMV, by light scattering or by using antigen-specific antibodies followed by a second fluorescent antibody (10). Previously, on traditional flow cytometry machines, the limit of detection was around 200-nm particles (5), and conventional flow cytometers could not differentiate between particles that differed by less than 100–200 nm (11). The recent application of flow cytometric methods to submicron virions, including Nipah virus and CMV, was a large step forward in establishment of new virological methods. Further, Junin virus was sorted using fluorescently labeled antibody to the viral glycoprotein (12), marking significant progress in the ability to sort individual infectious viral particles. These recent analyses were applied to larger viruses, all within the detectable limits of flow cytometry. Most of these studies were performed on viruses generated in vitro, although the most recent application of this technology utilized clinical CMV samples (10).

The technological advances in flow cytometry that have allowed for the evaluation of viruses and other biologically relevant small particles can be applied to the advancement of the HIV-1 field. We have previously demonstrated that we can sort individual HIV virions labeled with fluorescent membrane dyes (PKH26 and PKH67) (T. Musich et al., unpublished observations). While this staining method may be applicable to in vitro experimentation, it may prove too problematic to adapt for use on clinically relevant samples. Membrane stains might compromise the lipid bilayer as well as nonspecifically stain other membranous vesicles. Utilizing fluorochrome-conjugated antibodies directed toward HIV- and SIV-specific proteins and known cell-derived proteins incorporated into virions, we demonstrate here the ability to not only phenotypically identify viral quasispecies present in the serum and plasma of infected nonhuman primates and humans, but also to sort different populations from one another. Developing HIV envelope antigens that will elicit desired antibody responses has been a major goal of the vaccine field, and various approaches have made significant steps toward that end. As shown here, flow virometry can utilize antibodies to identify reactive virus in infected human plasma. Moving forward, there is the potential to identify and isolate antibodies bound to a patient's HIV-1 in vivo by sorting HIV-1 virions from infected plasma samples, facilitating a novel personalized immunological approach to an HIV-1 infection. While maintaining infectivity, virus can be sorted from archived clinical samples of importance for molecular, proteomic, and genomic characterization. We demonstrate the foundation for these analyses in the experimentation presented here.

Results

Sorting HIV derived from different cell types. In order to demonstrate that distinct HIV/SIV viral populations can be stained and sorted from each other using fluorescently conjugated antibodies, we first generated HIV-1 replication–incompetent virus with different phenotypes in cell lines. THP-1 human monocytic cells were used to generate Bal HIV-1. H9 human T cells were used to generate NL4.3 HIV-1. Bal is a CCR5-tropic virus, while NL4.3 is a CXCR4-tropic virus. The well-characterized phenotypes for these respective viruses allowed us to validate sorting of virions on an advanced flow cytometer, the Astrios EQ, using molecular techniques. We utilized a strategy that previously demonstrated the cellular origin of HIV-1 virions (13) and identified CD36 as being preferentially incorporated into virions originating from monocytes/macrophages, CD26 as being preferentially incorporated into virions originating from T cells, and CD44 as being preferentially incorporated into virions originating from both lymphoid and myeloid cells. Bal was left unstained or stained with anti-CD36 (Figure 1, A and B); similarly, NL4.3 was left unstained or stained with anti-CD26 (Figure 1, C and D). Supplemental Figure 1 (supplemental material available online with this article; https://doi.org/10.1172/jci.insight.90626DS1) shows the negligible staining observed with THP-1 and H9 uninfected cell supernatants. Bal and NL4.3 virions were then stained separately with anti-CD36 and anti-CD26, respectively, combined, and sorted (Figure 1E) or were combined, stained simultaneously

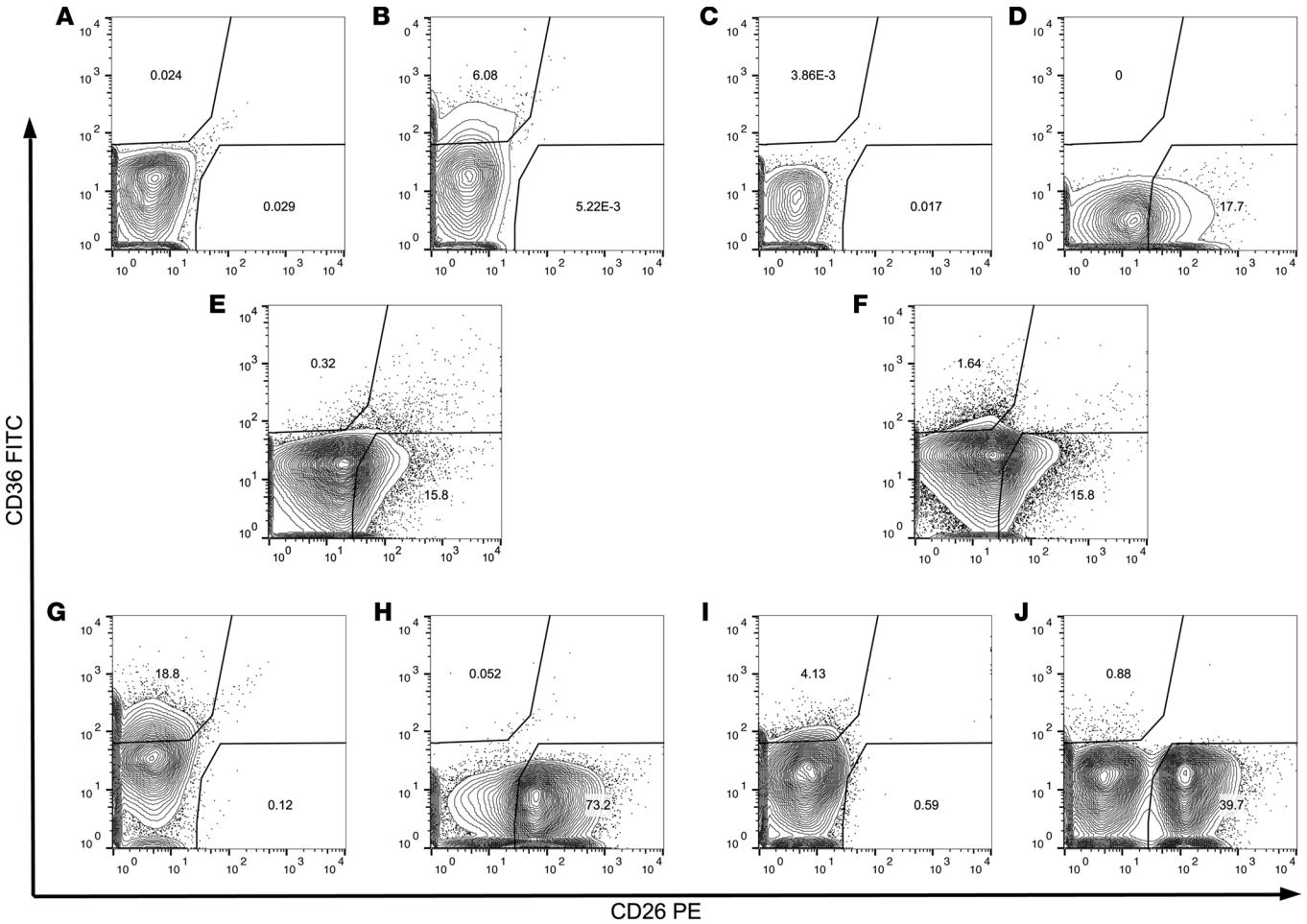

Figure 1. Sorting HIV derived from different cell types. Bal HIV-1 was made in THP-1 cells, and NL4.3 was made in H9 cells. (**A**) Unstained Bal. (**B**) Bal stained with anti-CD36. (**C**) Unstained NL4.3. (**D**) NL4.3 stained with anti-CD26. (**E**) Bal and NL4.3 were first stained separately with anti-CD36 and anti-CD26, respectively, and then combined and sorted. (**F**) Bal and NL4.3 were first combined and then stained at the same time with both anti-CD36 and anti-CD26. (**G**) Sorted CD36$^+$ population from **E** reanalyzed after sort. (**H**) Sorted CD26$^+$ population from **E** reanalyzed after sort. (**I**) Sorted CD36$^+$ population from **F** reanalyzed after sort. (**J**) Sorted CD26$^+$ population from **F** reanalyzed after sort. This figure represents 1 of 3 separate experiments.

with both antibodies, and sorted (Figure 1F). The reanalyzed sorted populations are shown in Figure 1, G–J, with sorted CD36$^+$ virus (Figure 1G) and sorted CD26$^+$ virus (Figure 1H) from the virus that was stained separately prior to mixing and the virus stained together after being mixed (Figure 1, I and J). The reanalysis of sorted populations that were stained separately (Figure 1, G and H) clearly resulted in a better reanalysis profile, with greater resolution and recovery than when stained together (Figure 1, I and J), and both yielded pure populations. These results demonstrated that this flow cytometric sorting technique could be applied to clinical samples, such as infected plasma or serum and potentially whole blood.

Sorted HIV maintains infectivity. The sorted virus obtained from the population that was mixed first and stained with both antibodies simultaneously was placed on U373 reporter cells expressing CD4 and either CCR5 or CXCR4 following reanalysis. This was done to not only ascertain the purity of the viral populations after sorting, but also to ensure that the virus was still infectious and intact following the sorting process. As expected based on viral tropism, the CD36$^+$ sorted virus only infected the CCR5-expressing cells (Figure 2A), without infecting the CXCR4$^+$ cells (Figure 2C). The CD26$^+$ sorted virus did not infect the cells expressing CCR5 (Figure 2B), but it did infect the CXCR4$^+$ cells (Figure 2D). This infectivity assay thus demonstrated that this sorting process yielded distinct viral populations that remained infectious, suggesting that these methods can be applied to clinical samples for evaluation of mixed viral quasispecies. We have previously shown the presence of HIV viral particles by electron microscopy (EM) (T. Musich et al., unpublished observations), following sorting of HIV Bal stained with a fluorescent membrane dye (Supplemental Figure 2), demonstrating the presence of intact virions following sorting by the techniques used here.

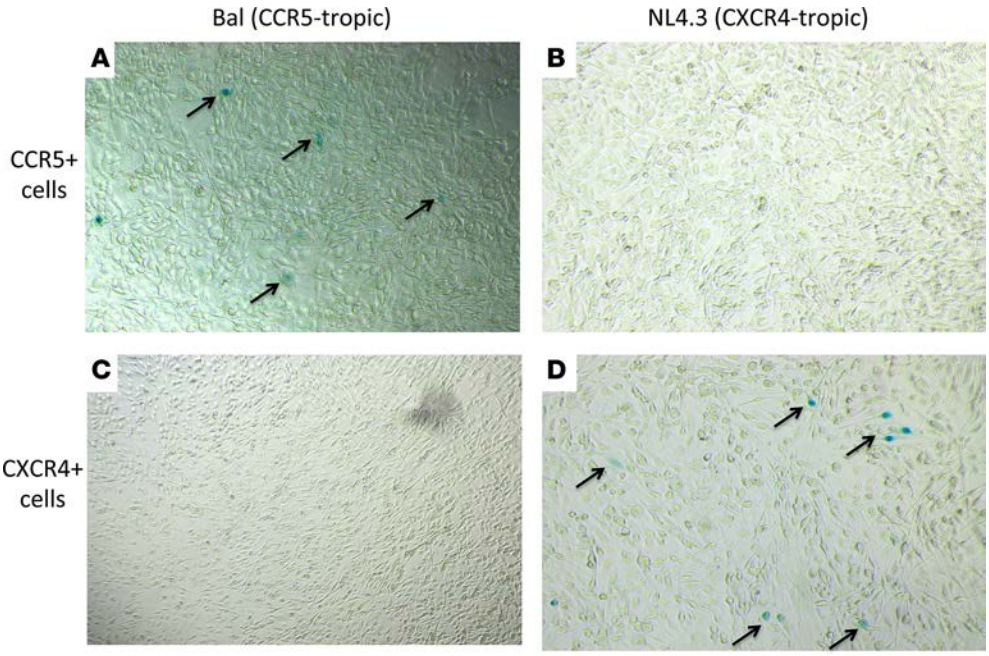

Figure 2. Sorted HIV-1 originating from different cell types maintains tropism and infectivity. Bal HIV-1 was made in THP-1 cells, and NL4.3 was made in H9 cells. These viral populations were mixed, stained together for CD36 and CD26, sorted from one another, and used to infect U373-MAGI-CCR5E cells (**A** and **B**) and U373-MAGI-CXCR4$_{CEM}$ cells (**C** and **D**). After 48 hours, cells were fixed and stained for β-galactosidase expression. Sorted Bal only infected CCR5$^+$ cells (**A**), and sorted NL4.3 only infected CXCR4$^+$ cells (**D**). Infected cells are tinted blue and marked with arrows. Original magnification, ×10.

Isotype staining of virions. Evaluating HIV-1 virions using flow cytometry is significantly different compared with evaluating cells, but certain principles are applicable to both. In order to ensure that the observed antibody binding to the virus was real and not simply nonspecific interaction, we compared the staining of the virus with antigen-specific antibody to staining with isotype controls. Presumably, not all virus is positive for the target cellular antigens, and, conversely, some nonviral particles may be positive for the targeted cellular antigens. However, as shown by infection of the U373 reporter cells (Figure 2), a proportion of the stained vesicles was made up of virions. Isotype staining of the pseudotyped virus used in Figures 1 and 2 demonstrated the background level of nonspecific staining (Figure 3, A and C), while antibody staining resulted in a clear fluorescent signal above the isotype background (Figure 3, B and D), enabling the proper evaluation of fluorescently stained virus. When analyzing virus from plasma, the difference between an isotype-stained virus (Figure 3E) and CD44-stained simian/human immunodeficiency virus (SHIV) from a highly infectious plasma sample of an infected rhesus macaque was readily apparent (Figure 3F). This plasma sample was obtained in May 2012 and remained frozen for over 3 years prior to being thawed and stained, demonstrating that this technique can easily be applied to archived clinical samples.

Quantification of SHIV sorted from stored plasma. The CD44$^+$ stained SHIV shown in Figure 3F was sorted from diluted plasma. 200,000 events were sorted and quantified in three ways before and after sort: by infectious titer on TZM-BL cells, by quantification of viral RNA, and by quantification of the viral core protein, p27 (Table 1). TZM-BL cells were used to titer the virus both from diluted plasma (Figure 4A) and from the sorted sample (Figure 4B), resulting in titers of 28,600 FFU/ml and 145 FFU/ml, respectively (0.5% of the original titer). The viral load of the plasma was originally quantified when the sample was frozen as 5×10^7 RNA copies/ml. The sample was again quantified both before and after sort, yielding 2.74×10^7 RNA copies/ml before sort and 1.9×10^5 RNA copies/ml after sort (~0.7%). Last, a p27 ELISA was performed on the fractions before and after sort, with the before sort fraction having 3,850 pg/ml of p27 and the sorted fraction having 16.6 pg/ml (~0.4%). All three methods of quantification yielded similar results, showing a recovery of approximately 0.5% of the input virus after sort. Importantly, this calculation is overly conservative, as it assumes all sorted events are virus. If it is assumed that less than 50% of the CD44$^+$ sorted events are virus, as many extracellular vesicles are also CD44$^+$, the sorting efficacy, as it relates to virus alone, increases dramatically.

Sorted SHIV is bound to viral-specific IgG in the infected animal. In light of the small return in the sorted fraction compared with the original amount of virus in the plasma, we hypothesized that much of the virus might already be bound to plasma Ig. Unstained plasma from the SHIV-infected macaque with a high viral load exhibited no autofluorescence (Figure 5A). The plasma was stained with anti-CD44, as in Figure 3F; sorted for CD44$^+$ virions (Figure 5B); and reanalyzed (Figure 5C). The reanalyzed and sorted virus was then either stained with an isotype control (Figure 5D) or stained with anti-monkey IgG (Figure 5E). Roughly one-third of the CD44$^+$ sorted virus was also positive for rhesus IgG, indicating that a substantial portion of the virus present in plasma was bound to antibodies. When uninfected plasma was analyzed in the same

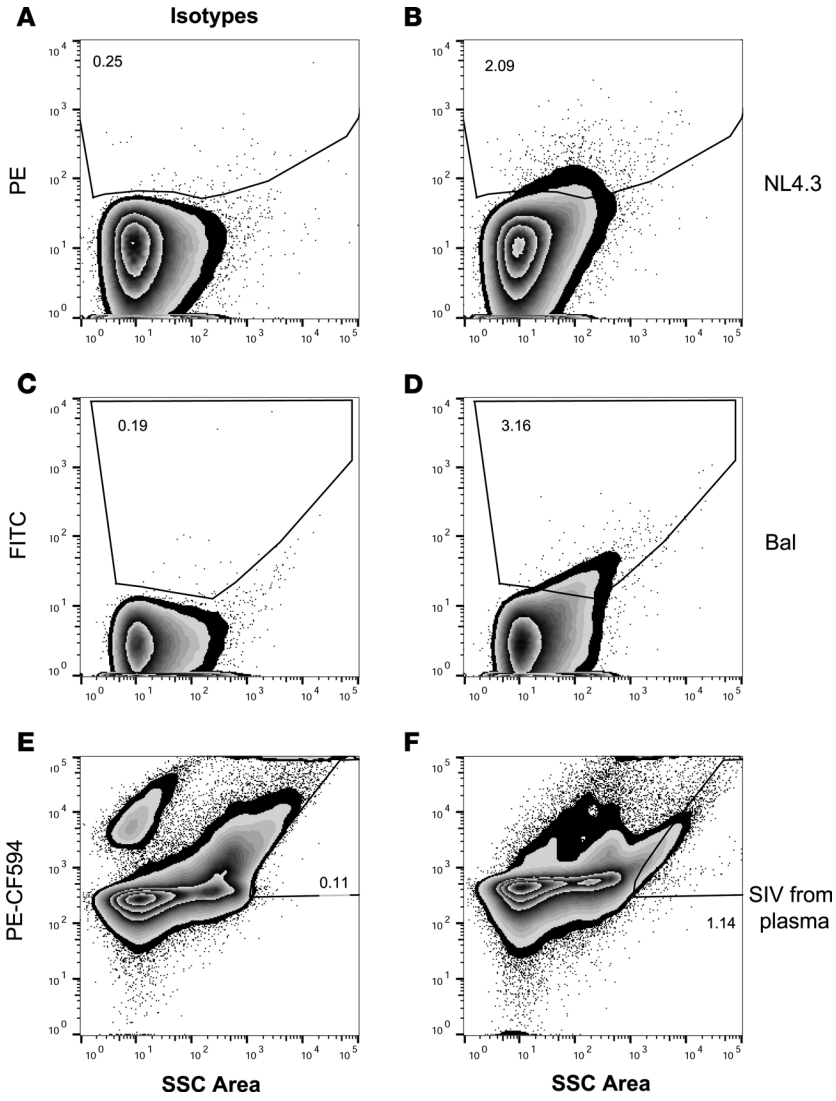

Figure 3. Isotype staining of cell line–derived HIV-1 and SHIV from plasma. (**A** and **B**) NL4.3 HIV-1 derived from H9 cells stained with (**A**) isotype control and (**B**) anti-CD26. (**C** and **D**) Bal HIV-1 derived from THP-1 cells stained with (**C**) isotype and (**D**) anti-CD36. (**E** and **F**) High viral load plasma (>10^6 RNA copies/ml) from SHIV-infected rhesus macaque P967 stained with (**E**) isotype and (**F**) anti-CD44. This CD44$^+$ stained SHIV was then sorted from the infectious plasma. This figure represents 1 of 3 separate experiments.

manner, markedly fewer CD44$^+$ vesicles were observed, and they lacked bound IgG (Supplemental Figure 3). We may be able to capitalize on this in the future by isolating antibodies that bind to viral quasispecies present in the blood.

HIV-1 virus sorted from infected human plasma using two broadly neutralizing antibodies. The viral sorting technique was then applied to infectious human plasma. Two broadly neutralizing antibodies directed to different epitopes on gp120, PG9, which recognizes a glycopeptide epitope located in the V1–V2 region (14), and VRC01, which recognizes the CD4-binding site (15), were conjugated to fluorochromes and used to sort virus for further downstream analysis. The plasma is shown unstained (Figure 6A), stained with PG9 only (Figure 6B), and stained with VRC01 only (Figure 6C). The plasma was also stained simultaneously with PG9 and VRC01 (Figure 6D), and the three populations from the single subject shown were sorted for downstream analysis. Roughly three times more double-stained virions were detected (161,000) than virions stained with PG9 (52,000) or VRC01 (48,000) only. Representative staining with isotype controls is shown in Supplemental Figure 4.

Genetic and proteomic analysis of HIV-1 sorted from human plasma. The sorted populations of virus were then analyzed genetically and using proteomics. Sequence data were obtained using input plasma virus and the sorted viral populations (Figure 6D) as well as virus sorted on a duplicate sample using 7B2-AAA, a non-neutralizing antibody targeting a gp41 epitope (16), to detect virions that had perhaps shed gp120 and also to attempt to identify a different viral quasispecies (data not shown). Sequences were obtained using a single-genome sequencing approach and analyzed phylogenetically (Figure 7). Most of the sorted virus appears very similar in sequence to the input virus, indicating isolation of genetically overlapping genomes, regardless of which binding antibody (PG9, VRC01, or 7B2-AAA) was used. Apparently, there was sufficient cross reactivity of these antibodies with the major viral lineages so that a distinct viral quasispecies was not detected. Interestingly, 5 input virus sequences at the root of the tree were notably different than the rest of the tree and

Table 1. SHIV quantification from sorted infectious plasma

	TZM-BL titer (FFU/ml)	RNA (copies/ml)	p27 ELISA (pg/ml)
Plasma input	28,600	2.74×10^7	3,849.97
CD44 sorted virus	145	1.9×10^5	16.63
Sorted virus (% of input)	0.51	0.69	0.43

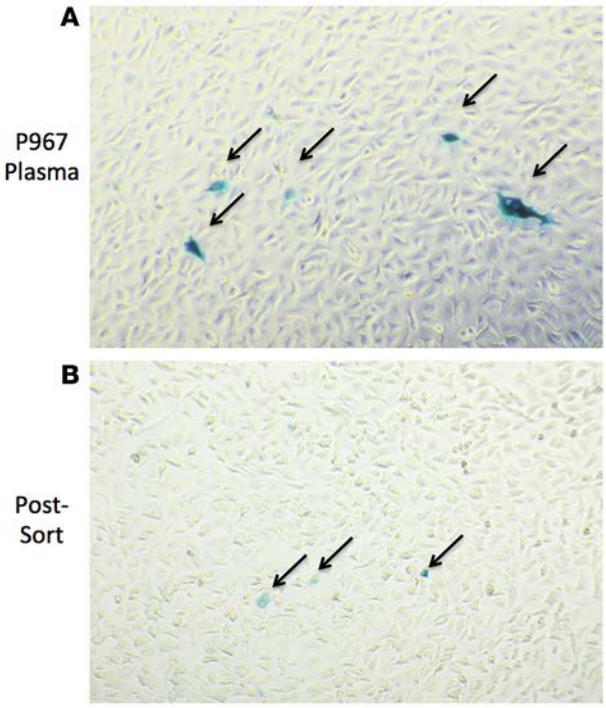

Figure 4. SHIV sorted from plasma is infectious. TZM-BL cells were used to titer virus in plasma from infected animal P967 before and after sort. 48 hours after the cells were inoculated, they were stained for the expression of β-galactosidase. Infected cells are tinted blue and marked with arrows. (**A**) The image illustrates that the infected plasma contained infectious virus. (**B**) The image demonstrates that virus sorted from the plasma ($CD44^+$ virus) using the methods described herein maintains infectivity. The titers are quantified in Table 1. Original magnification, ×10.

were not represented in any of the sorted samples. We conclude that there was sufficient reactivity of the antibodies used for sorting to allow isolation of most viral genomes within the dominant cluster of the phylogenetic tree.

Mass spectrometry analysis performed on sorted samples (Figure 6D) confirmed the presence of HIV-specific peptides. Peptides detected in $PG9^+$, $VRC01^+$, and/or $PG9^+VRC01^+$ populations are shown in Table 2. Several of the Env peptide sequences identified were largely homologous, with deduced sequences obtained by genetic analysis of the same sorted samples. In addition to Env peptides, Gag-Pol and Vpr peptides were also detected. Unlike genomic analysis, no amplification step is used in proteomic analysis, and more sorted material was likely necessary in order to identify a greater number of viral proteins or cellular proteins incorporated into the virions. Additional nonviral proteins were identified in the sorted samples, largely those found in serum or plasma (data not shown).

Discussion

Here, we demonstrate that virus both in cell culture and plasma can be stained for viral-specific or cellular antigens incorporated into virions and sorted using advanced flow cytometric techniques. Subsequent analysis of such sorted populations can provide very insightful information, not only for virology in general, but specifically for the further study of HIV-1 and attempts at prevention or eradication. In sorting virus generated in vitro from two different cell types, we have shown that we can utilize cell-derived incorporated proteins to stain virus or other cell-derived vesicles. Using this methodology, we can verify proteins that are incorporated into the virus membrane and determine at what frequency they are incorporated. A number of proteins have been detected in the membrane of HIV-1 (17). Utilization of flow cytometry to sort HIV-1 quasispecies present in plasma expressing a certain cell-derived protein may provide new insights into how this incorporated protein affects the virus. Additionally, using previously described proteins that indicate the cell type of origin for virus

Table 2. Peptides detected by mass spectrometry analysis of sorted HIV-1

Sample[A]	Gene	Residues	Annotated sequence
VRC01 and mix	Env	9–45	NYQRLWRWGTMLLGMLMICSAAENLWVTVYYGVPVWK
Mix	Env	16–58	WGTLLLGMLMICSATEKLWVTVYYGVPVWKEATTTLFCASDAR
PG9 and mix	Env	16–58	WGTMLLGMLMIVSAAENLWVTVYYGVPVWKEATTTLFCASDAR
Mix	Env	97–120	NNMVEQMQEDIISLWDQSLKPCVK
PG9 and mix	Env	97–120	NNMVEQMQEDVINLWDQSLKPCVK
Mix	Env	303–324	KSIHIGPGRAFYTTGEIIGDIR
PG9	Env	454–473	DGGTNVTNDTEVFRPGGGDMR
Mix	Gag-pol	306–331	AEQASQDVKNWMTETLLVQNANPDCK
Mix	Gag-pol	315–359	NWMTETLLVQNANPDCKTILKALGPAATLEEMMTACQGVGGPGHK
VRC01	Gag-pol	464–482	ELQVWGGENNSLSEAGADR
VRC01	Gag-pol	502–532	IGGQLKEALLDTGADDTVLEEMNLPGRWKPK
PG9	Gag-pol	511–536	EALLDTGADDTVLEEMNLPGK
Mix	Gag-pol	975–1010	FKLPIQKETWEAWWTEYWQATWIPEWEFVNTPPLVK
Mix	Vpr	13–36	EPYNewTLELLEELKNEAVRHFPR
VRC01	Vpr	28–62	NEAVRHFPRIWLHSLGQYIYETYGDTWAGVEAIIR

[A]Mix represents the $PG9^+VRC01^+$ sorted population. Virions sorted using the 7B2-AAA monoclonal antibody were not included in the analysis.

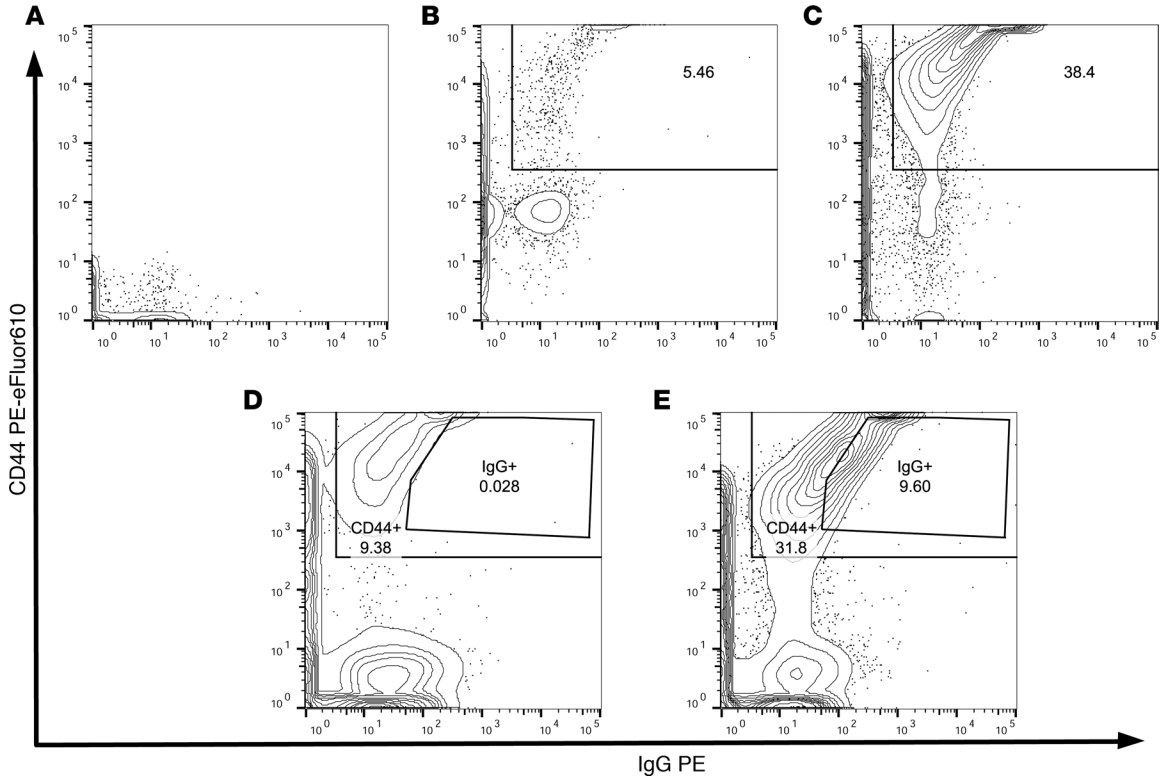

Figure 5. SHIV sorted from infectious plasma is bound to IgG generated by the infected animal. (**A**) Unstained serum has no autofluorescence. (**B**) Infected serum stained with anti-CD44 sorted for CD44$^+$ virus. (**C**) Reanalyzed sorted CD44$^+$ virus. (**D**) CD44$^+$ virus sorted from serum stained with isotype control and (**E**) anti-rhesus IgG. This figure represents 1 of 3 separate experiments.

generation (13), we can further evaluate the contribution of the cell of origin to a budding virion in a clinically relevant sample. These cellular protein markers will certainly be found in other budding vesicles, some of similar size to HIV-1. However, by using well-defined HIV-1 molecular techniques and HIV-1–specific proteins, we can separate out the background contribution of these vesicles from the viral population. Such an approach is demonstrated by our application of sorted virus from THP-1 cells and H9 cells to U373 coreceptor-specific cells in order to illustrate infectivity and relative purity of the sort (Figure 2). Any additional sorted nonviral vesicles that also expressed CD26 or CD36 would not have affected the assay results.

Because flow cytometry is a technology in which results can easily be misinterpreted, application of this technique requires rigorous identification of virions. Using isotype controls (Figure 3), we demonstrated effective staining and evaluation of virus above background. However, the margin of error when comparing infectious plasma stained with anti-CD44 versus an isotype control is very small (Figure 3, E and F). Conservative gating is necessary, and while that markedly decreases the amount of virus available for analysis, it ensures accuracy in sorting stained virus from infectious plasma/serum. The yield obtained here in sorted samples was low: roughly 0.5%–0.7% of the input virions, depending on the method of quantification. Thus, sorting of a highly infectious plasma/serum sample containing 10^6 virions would yield approximately 5,000 virions. This indicates that, given the current limits of the

Table 3. Antibodies used for flow virometry

Antigen	Fluorochrome	Clone	Host species	Isotype	Supplier
CD26	PE	2A6	Mouse	IgG_1,κ	eBioscience
CD36	FITC	FA6-152	Mouse	IgG_1,κ	Stemcell
CD44	PE-eFluor610	IM7	Mouse	IgG2b,κ	eBioscience

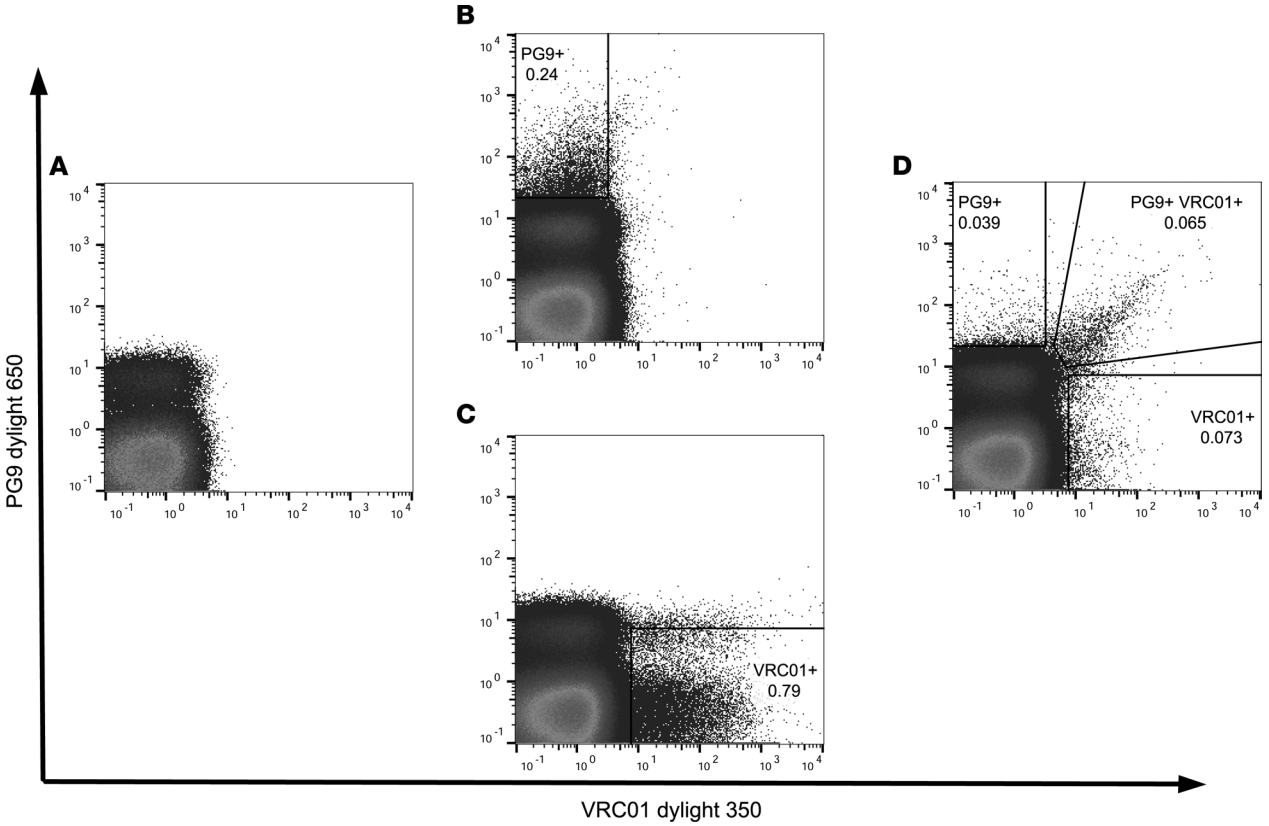

Figure 6. HIV-1 virus sorted from infected human plasma using two broadly neutralizing antibodies. (**A**) Unstained plasma has no autofluorescence. (**B**) Infected plasma stained with PG9. (**C**) Infected plasma stained with VRC01. (**D**) Infected plasma stained simultaneously with PG9 and VRC01. The 3 populations shown were subsequently sorted and analyzed. This figure represents 1 of 5 separate experiments.

technology, only samples with viral titers of 10^4–10^5 per ml or greater would be worth evaluating with this current approach without pre-enrichment. The relatively low yield may result from the actual sorting process itself, as the virus is subjected to both high pressure and an imperfect sorting medium. Additionally, virus is lost during the stringent dropwise sorting process. Further, it is likely that noninfectious virus that also possesses p24 and RNA is also sorted along with intact virus, affecting accurate quantification of the sorted populations, as unsorted HIV preparations can exhibit infectious to noninfectious ratios of up to 1:60,000 (18). This might explain why the sorted viral titer, as calculated based on infectivity, was lower than the expected titer, as estimated based on RNA quantification (Table 1). Further, the titer may also be influenced by extracellular vesicles that are $CD44^+$ that are cosorted when using CD44-based selection. Sorting efficiency should be improved as the usage of these techniques expands. By using smaller nozzle sizes, it is feasible that one can effectively sort more particles in a shorter period of time, potentially resulting in logarithmic improvement in virus yield. This is particularly important with regard to HIV-infected individuals in developed countries in which antiretroviral therapy generally maintains viral burdens at low levels. However, currently, given a sample with enough viral particles, this limitation ceases to be an issue.

Viral-specific antibodies, naturally generated in vivo during infection and bound to the virus in plasma/serum, are also a critical factor that may affect the viral material that can be obtained with this sorting strategy. A large amount of HIV-specific antibody is present in the blood of infected individuals. Potentially 100 μg/ml of HIV-specific IgG is available to bind free HIV (19). As the virus evolves and mutates to escape the antibody response, these antibodies may still weakly bind and associate with various virions present in the blood (20). We showed that roughly one-third of the sorted virus was already bound to IgG in the plasma prior to sorting (Figure 5E). While this might detract overall from the efficiency we are able to obtain, it also presents the opportunity for isolation and potential analysis of these antibodies. Isolation might be achieved by low-pH separation of the antibody bound to

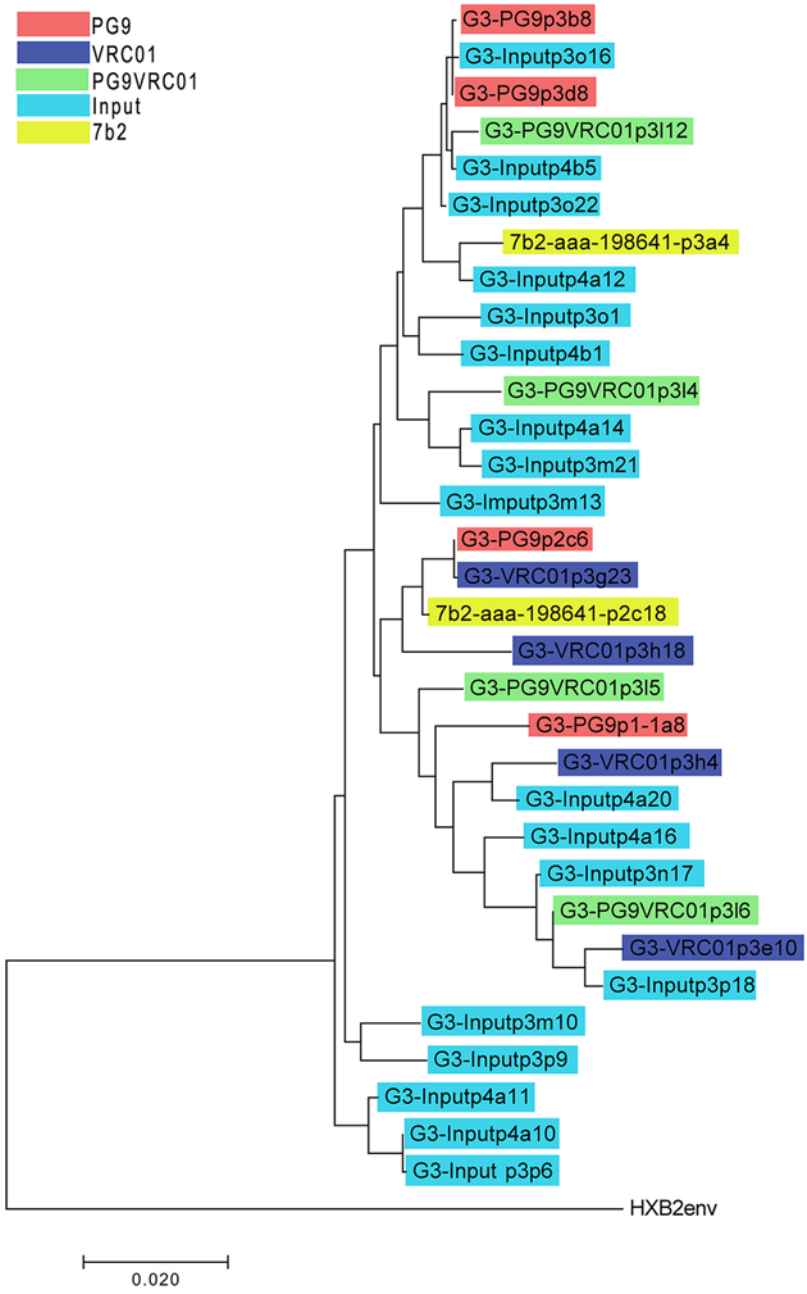

Figure 7. Phylogenetic tree of sorted HIV-1 from infectious patient plasma. Molecular phylogenetic analysis by the maximum likelihood method was conducted on aligned input plasma and sorted PG9$^+$, VRC01$^+$, PG9$^+$VRC01$^+$, and 7B2-AAA$^+$ populations. The evolutionary history was inferred by using the maximum likelihood method based on the Tamura-Nei model (33). The tree with the highest log likelihood (–8,368.3579) is shown. Initial tree(s) for the heuristic search were obtained automatically by applying the neighbor joining and BioNJ algorithms to a matrix of pairwise distances estimated using the maximum composite likelihood approach and then selecting the topology with superior log likelihood value. The tree is drawn to scale, with branch lengths measured in the number of substitutions per site. The analysis involved 33 nucleotide sequences. All positions containing gaps and missing data were eliminated. There were a total of 2,492 positions in the final data set. Evolutionary analyses were conducted in MEGA71 (34).

the virus. Analysis of the bound antibodies would prove quite difficult, but might be achieved by mass spectrometry. This approach requires further testing and optimization.

While expansion of the techniques described here promises intriguing opportunities and advancements for the HIV field, sorting virus from clinically relevant plasma samples was our primary focus. We utilized two broadly neutralizing antibodies that bound different epitopes, PG9, which recognizes a V1/V2 epitope (14), and VRC01, which recognizes a CD4-binding site epitope (15). We demonstrated clearly that we can currently sort up to three populations effectively (Figure 6). The Astrios EQ can potentially sort multiple different populations, and as this technique is developed and efficacy improves, we may be able to take advantage of this flexibility. Given our current limitations, the fewer the sorting parameters, the greater the yield in sorted populations. In general, however, any antibody that binds HIV/SIV could be used to sort virus from infectious serum or plasma.

The proteomic (Table 2) and genetic data (Figure 7) demonstrate that sorting and analysis of viral populations can be readily applied to archived clinical samples of interest. The antibodies used here for sorting broadly recognized the virus populations present in the patient plasma and did not discriminate different quasispecies. These antibodies are both very broad, recognizing almost all clade B Envs, and neutralizing 80% (PG9) to 96% (VRC01) of them (21, 22). The plasma was obtained from a patient who had stopped HAART, resulting in considerable viral expansion, up to a level of 10^6 HIV RNA copies/ml. Utilizing genetic sequencing before and after sort, we were able to capture the genetic diversity present in this clinical sample. Given a more diverse starting viral quasispecies with a greater spectrum of antibody epitopes, the differences observed might have been greater. This possibility could be addressed certainly using an animal model, potentially a cohort of superinfection in which significantly different viruses are represented, or by sorting plasma virus from an HIV-1–infected patient prior to any therapy.

This methodology for sorting infectious and clinically relevant HIV from patient material may be preferable to the other methods previously described. Sorting virus using magnetic beads certainly works, but it requires dual staining or binding of bead-conjugated antibodies. The magnetic nanoparticles used may be

bound to multiple antibodies, so small clusters of virions could be misrepresented as one virus. Additionally, most previous methods for analysis of HIV using flow cytometric techniques have relied on fluorescent triggering. Our method was able to trigger on these small particles using side scatter, allowing for better small-particle resolution and the potential to capture not only HIV virions that are bound to the desired antibodies, but importantly the ones that are not recognized by the antibodies used. These techniques can be accomplished using conventional, commercially available antibodies and performed directly on patient material, whether it is fresh or frozen, whereas past fluorometric staining methods could not readily be applied to archived serum or plasma without an intermediate purification step. Taken together, the benefits of the method described here favor its continued usage and refinement moving forward.

In summary, by applying advanced flow cytometry techniques used for addressing nanoscale particles, we were able to sort clinically relevant HIV from archived patient plasma. Any desired antibody that recognizes HIV/SIV can be used to isolate populations of virus from infected plasma or serum. Not only can the virus be analyzed using the flow cytometer, the sorted virus can be further utilized for any desired downstream characterization, whether it be genetic, proteomic, or conventional molecular assays. These capabilities have the potential to contribute significantly to antigen design for the HIV vaccine field as well as to aid clinicians directly in personalizing treatment approaches for HIV-infected individuals.

Methods

Cell culture. The U373-MAGI-CXCR4$_{CEM}$ (catalog 3596) and U373-MAGI-CCR5E (catalog 3597) cell lines were obtained from the NIH AIDS Reagent Program, Division of AIDS, National Institute of Allergy and Infectious Diseases, and cultured in 90% DMEM; 10% fetal bovine serum; 0.2 mg/ml G418; 0.1 mg/ml hygromycin B; and 1.0 μg/ml puromycin. 293T and TZM-BL cells (23) were cultured in DMEM with 5% fetal bovine serum.

Preparation of replication-incompetent virus. Replication-incompetent pseudovirions were prepared as previously described (24). Briefly, 1.25 μg of pSVIIIenv or pcDNA3.1TOPO plasmid carrying complete envelope sequences were cotransfected by using lipofectamine into H9 and THP-1 cells, together with 1.25 μg of pNL43 that carried a premature stop codon in the envelope (Env$^+$). Pseudovirions were harvested from these cell lines 48 hours after transfection, clarified by low-speed centrifugation, aliquoted into 0.5-ml portions, and snap frozen in liquid nitrogen.

Antibodies used for staining. Commercial antibodies utilized in this study are listed in Table 3. PG9 (21), VRC01 (22), and 7B2-AAA (16, 25) were obtained from the NIH AIDS Reagent Program. These monoclonal antibodies (mAbs) were custom conjugated using Lightning-link Rapid Dylight-650 and Dylight-350 kits (Innova Biosciences). Human IgG1 (Abcam) was used as an isotype control and custom conjugated in the same manner as the aforementioned mAbs. Appropriate mouse isotype controls were used when needed (BD Biosciences).

HIV-positive plasma. Archived plasma obtained from 3 HIV-infected individuals with viral loads ranging from 3.3×10^5 to 2.9×10^6 were used for sorting. Data from patient P198641 are shown in Figures 6 and 7 as well as Table 2. Patient 198641 is a man who was diagnosed as HIV positive in June 2012; a month later, he was diagnosed as having multicentric Castleman disease and primary effusion lymphoma. The patient developed drug resistance to efavirenz and nevirapine. At the time of plasma collection in November 2013, the patient was nonadherent to antiretrovirals, with a CD4$^+$ count of 64.

Archived plasma with a high viral load was obtained from a rhesus macaque infected with SHIV$_{SF162P4}$ (26). Uninfected plasma was obtained prior to vaccination from a macaque enrolled in a current study at the National Cancer Institute.

Virus staining and flow virometry. For EM analysis, PKH26 (Sigma-Aldrich) was used to stain 293T-derived HIV pseudovirions. Briefly, virus was diluted 4-fold using the diluent provided by the manufacturer (Sigma-Aldrich). Immediately prior to staining, the PKH dye was diluted 25-fold using the same diluent. The diluted virus was added to the diluted PKH and immediately mixed by pipetting. After incubating for 5 minutes while occasionally inverting the tube to mix, an equal volume of RPMI with 10% FBS was added to the virus-PKH mixture. The stained virus was then centrifuged at 15,000 *g* for 20 minutes and resuspended in 0.1-μm filtered RPMI 1640 medium for sorting, as described below. Virions before and after sort were fixed with glutaraldehyde for EM analysis performed by the NCI Frederick Electron Microscopy Core.

Virus was stained with the antibodies listed in Table 3 or those described herein for 30 minutes at room temperature. Plasma and sera (1-ml samples) were stained after high-speed centrifugation (>80,000 *g* for 20

minutes) and resuspension of the pellet in 50–100 μl 0.1-μm filtered PBS. Unbound antibodies were washed away by centrifugation at 15,000–80,000 *g* for 20 minutes. Stained virus in the pellet was suspended in 150 μl 0.1-μm filtered PBS, and 10-fold dilutions were analyzed on a modified Beckman Coulter Astrios EQ using a 70-μm nozzle. The dual-PMT forward scatter detector assembly was configured to direct all FSC light collection to one FSC detector, with no inline neutral density filter, and without a mask. Drop-drive frequency was 90–95kHz, with a plate voltage of 3,000 and an amplitude of 8–16 volts to remove drop-drive noise by setting a drop break-off point as far below the laser interrogation points as possible, while maintaining a stable stream and break-off point. The 561-SSC threshold was set to avoid as much background as possible, with a minimal background rate (<1,000 events per second). Sorting was performed in purity mode. For more detailed information regarding the MoFlo Astrios EQ, please refer to refs. 27 and 28.

Virus titration and quantification. U373-MAGI cells or TZM-BL cells (2.5×10^4 per well in a 48-well plate) were set up the day prior to infection in the medium described above. Virus was then added to plated cells and allowed to incubate for 48 hours. Medium was removed, and cells were washed once with PBS. 0.5 ml PBS/0.5% glutaraldehyde was added to each well and incubated at 4°C for 8–10 minutes. PBS/glutaraldehyde was removed, and cells were washed once with PBS. 200 μl of PBS containing 0.5 mg/ml X-Gal (5-bromo-4-chloro-3-indolyl-beta-D-galacto-pyranoside), 3 mM potassium ferricyanide, 3 mM potassium ferrocyanide, and 1 mM magnesium chloride was added per well. The plate was incubated at room temperature for 4 hours, and then the substrate was replaced with PBS/0.1% sodium azide and foci of infection were quantified. The p27 ELISA was conducted using a kit from Advanced Bioscience Laboratories Inc. SHIV RNA quantification was performed by the quantitative nucleic acid sequence–based amplification assay (29, 30).

Single-genome amplification. Single-genome amplification followed by direct sequencing (single-genome sequencing) of the Env gene was used to eliminate Taq induced errors and in vitro recombination as described previously (31). Briefly, viral RNA was isolated from plasma using a QIAamp viral RNA kit (Qiagen). Reverse transcription of RNA to single-stranded cDNA was performed using SuperScript III Reverse Transcriptase according to the manufacturer's recommendations (Invitrogen). In brief, a cDNA reaction of 1× RT buffer, 0.5 mM of each dNTP, 5 mM DTT, 2 U/ml RNaseOUT (RNase [recombinant ribonuclease] inhibitor), 10 U/ml SuperScript III Reverse Transcriptase, and 0.25 mM antisense primer EnvB3out 5′-TTGCTACTTGTGATTGCTCCATGT-3′ was used. RNA, primers, and dNTPs were heated at 65°C for 5 minutes and then chilled on ice for 1 minute. Then, the entire reaction was incubated at 50°C for 60 minutes, followed by 55°C for additional 60 minutes. Finally, the reaction was heat inactivated at 70°C for 15 minutes and then treated with 1 μl RNase H at 37°C for 20 minutes. Then, cDNA templates were serially diluted until only a fraction (~25%) of amplicons were PCR positive with the following PCR conditions: PCR amplification was carried out using the Platinum Taq (Invitrogen) with 1× buffer, 2 mM $MgCl_2$, 0.2 mM of each dNTP, and 0.025 U/μl Platinum *Taq* polymerase; the appropriate primers were added at a concentration of 0.2 μM. The primers for the first-round PCR were EnvB5out 5′-TAGAGCCCTGGAAGCATCCAGGAAG-3′ and EnvB3out 5′-TTGCTACTTGTGATTGCTCCATGT-3′. The primers for the second-round PCR were EnvB5in 5′-CACCTTAGGCATCTCCTATGGCAGGAAGAAG-3′ and EnvB3in 5′-GTCTCGAGATACTGCTCCCACCC-3′. The cycler parameters were 94°C for 2 minutes, followed by 35 cycles of 94°C for 15 seconds, 55°C for 30 seconds, and 68°C for 4 minutes, followed by a final extension of 68°C for 10 minutes. The product of the first-round PCR (1 μl) was subsequently used as a template in the second-round PCR under same conditions but with a total of 45 cycles. All PCR-positive amplicons were directly sequenced using BigDye Terminator chemistry (Applied Biosystems). Any sequence with evidence of double peaks was excluded from further analysis. Env sequences were aligned with ClustalW, and phylogenetic trees were constructed using the neighbor joining method.

Mass spectrometry. Viral pellets were fractionated by SDS-PAGE, and protein bands were then in-gel digested with trypsin (Sigma-Aldrich) overnight at 37°C, as described previously (32). Extracted peptides were separated on a 75 μm × 15 cm, 2 μm Acclaim PepMap reverse-phase column (Thermo Scientific) coupled to an UltiMate 3000 RSLCnano HPLC (Thermo Scientific), followed by online analysis by tandem mass spectrometry using a Thermo Orbitrap Fusion mass spectrometer. Parent full-scan mass spectra were collected in the Orbitrap mass analyzer at 120,000 FWHM resolution; isolated ions were fragmented by HCD (normalized energy 32%, stepped ±3%), and the product ions were analyzed in the ion trap. Proteome Discoverer 2.0 (Thermo) was used to search the data against human and HIV-1 proteins from

the UniProt database using SequestHT. The search was limited to tryptic peptides, with maximally two missed cleavages allowed. Cysteine carbamidomethylation was set as a fixed modification; methionine oxidation was set as a variable modification. The precursor mass tolerance was 10 ppm; the fragment mass tolerance was 0.6 Da. The Percolator node was used to score and rank peptide matches using a 1% false discovery rate.

Study approval. All patients signed informed consent for the NCI IRB-approved protocol (NCT00006518). Plasma was obtained from rhesus macaques housed and maintained at Advanced Bioscience Laboratories Inc. or the NIH Animal Facility according to the standards of the American Association for Accreditation of Laboratory Animal Care, following practices recommended in the *Guide for the Care and Use of Laboratory Animals* (National Academies Press. 2011.). All procedures were approved by the Institutional Animal Care and Use Committees of Advanced Bioscience Laboratories, Inc. and the National Cancer Institute, respectively, prior to implementation.

Author contributions

TM designed and performed experiments, analyzed data, and wrote the paper; JCJ developed the nanoscale fluorescence-activated cytometric cell sorting method; JCJ and TD aided with experimental design and interpretation and edited the paper; BFK and LMMJ performed experiments and edited the paper; RY and TSU provided patient samples and clinical correlation and edited the paper; and MRG supervised the project and wrote the paper.

Acknowledgments

We would like to thank Karen Aleman for her help with the clinical samples used in this study and Stefanie Musich for her graphical help in preparing this manuscript. The following reagents were obtained through the NIH AIDS Research and Reference Reagent Program, Division of AIDS, National Institute of Allergy and Infectious Diseases: anti-HIV-1 gp120 monoclonal PG9; anti-HIV-1 gp120 monoclonal VRC01 from John Mascola; HIV-1 gp120 mAb 7B2-AAA from Barton F. Haynes and Hua-Xin Liao; and U373-MAGI-CCR5E and U373-MAGI-CXCR4$_{CEM}$ cells from Michael Emerman. This work was supported by the Intramural Research Program of the NIH, National Cancer Institute, and contract HHSN261200800001E. The content of this publication does not necessarily reflect the views or policies of the Department of Health and Human Services, nor does mention of trade names, commercial products, or organizations imply endorsement by the US government.

Address correspondence to: Marjorie Robert-Guroff, NIH, NCI, Vaccine Branch, 41 Medlars Drive, Building 41, Room D804, Bethesda, Maryland 20892-5065, USA. Phone: 301.496.2114; E-mail: guroffm@mail.nih.gov.

TD's present address is: Immatics US Inc., Houston, Texas, USA.

1. Hercher M, Mueller W, Shapiro HM. Detection and discrimination of individual viruses by flow cytometry. *J Histochem Cytochem*. 1979;27(1):350–352.
2. Brussaard CP, Marie D, Bratbak G. Flow cytometric detection of viruses. *J Virol Methods*. 2000;85(1-2):175–182.
3. Loret S, El Bilali N, Lippé R. Analysis of herpes simplex virus type I nuclear particles by flow cytometry. *Cytometry A*. 2012;81(11):950–959.
4. Steen HB. Flow cytometer for measurement of the light scattering of viral and other submicroscopic particles. *Cytometry A*. 2004;57(2):94–99.
5. van der Pol E, van Gemert MJ, Sturk A, Nieuwland R, van Leeuwen TG. Single vs. swarm detection of microparticles and exosomes by flow cytometry. *J Thromb Haemost*. 2012;10(5):919–930.
6. Nolan JP, Stoner SA. A trigger channel threshold artifact in nanoparticle analysis. *Cytometry A*. 2013;83(3):301–305.
7. Arakelyan A, Fitzgerald W, Margolis L, Grivel JC. Nanoparticle-based flow virometry for the analysis of individual virions. *J Clin Invest*. 2013;123(9):3716–3727.
8. Zicari S, et al. Evaluation of the maturation of individual Dengue virions with flow virometry. *Virology*. 2016;488:20–27.
9. Landowski M, Dabundo J, Liu Q, Nicola AV, Aguilar HC. Nipah virion entry kinetics, composition, and conformational changes determined by enzymatic virus-like particles and new flow virometry tools. *J Virol*. 2014;88(24):14197–14206.
10. Vlasak J, Hoang VM, Christanti S, Peluso R, Li F, Culp TD. Use of flow cytometry for characterization of human cytomegalovirus vaccine particles. *Vaccine*. 2016;34(20):2321–2328.
11. Lacroix R, et al. Standardization of platelet-derived microparticle enumeration by flow cytometry with calibrated beads: results of the International Society on Thrombosis and Haemostasis SSC Collaborative workshop. *J Thromb Haemost*.

2010;8(11):2571–2574.
12. Gaudin R, Barteneva NS. Sorting of small infectious virus particles by flow virometry reveals distinct infectivity profiles. *Nat Commun*. 2015;6:6022.
13. Lawn SD, Roberts BD, Griffin GE, Folks TM, Butera ST. Cellular compartments of human immunodeficiency virus type 1 replication in vivo: determination by presence of virion-associated host proteins and impact of opportunistic infection. *J Virol*. 2000;74(1):139–145.
14. McLellan JS, et al. Structure of HIV-1 gp120 V1/V2 domain with broadly neutralizing antibody PG9. *Nature*. 2011;480(7377):336–343.
15. Li Y, et al. Mechanism of neutralization by the broadly neutralizing HIV-1 monoclonal antibody VRC01. *J Virol*. 2011;85(17):8954–8967.
16. Santra S, et al. Human non-neutralizing HIV-1 envelope monoclonal antibodies limit the number of founder viruses during SHIV mucosal infection in rhesus macaques. *PLoS Pathog*. 2015;11(8):e1005042.
17. Ott DE. Cellular proteins detected in HIV-1. *Rev Med Virol*. 2008;18(3):159–175.
18. Piatak M, et al. High levels of HIV-1 in plasma during all stages of infection determined by competitive PCR. *Science*. 1993;259(5102):1749–1754.
19. Mestecky J, et al. Paucity of antigen-specific IgA responses in sera and external secretions of HIV-type 1-infected individuals. *AIDS Res Hum Retroviruses*. 2004;20(9):972–988.
20. Wei X, et al. Antibody neutralization and escape by HIV-1. *Nature*. 2003;422(6929):307–312.
21. Walker LM, et al. Broad and potent neutralizing antibodies from an African donor reveal a new HIV-1 vaccine target. *Science*. 2009;326(5950):285–289.
22. Wu X, et al. Rational design of envelope identifies broadly neutralizing human monoclonal antibodies to HIV-1. *Science*. 2010;329(5993):856–861.
23. Wei X, et al. Emergence of resistant human immunodeficiency virus type 1 in patients receiving fusion inhibitor (T-20) monotherapy. *Antimicrob Agents Chemother*. 2002;46(6):1896–1905.
24. Musich T, et al. A conserved determinant in the V1 loop of HIV-1 modulates the V3 loop to prime low CD4 use and macrophage infection. *J Virol*. 2011;85(5):2397–2405.
25. Zhang W, Godillot AP, Wyatt R, Sodroski J, Chaiken I. Antibody 17b binding at the coreceptor site weakens the kinetics of the interaction of envelope glycoprotein gp120 with CD4. *Biochemistry*. 2001;40(6):1662–1670.
26. Thomas MA, et al. HIV-1 CD4-induced (CD4i) gp120 epitope vaccines promote B and T-cell responses that contribute to reduced viral loads in rhesus macaques. *Virology*. 2014;471-473:81–92.
27. MoFlo Astrios EQ. Beckman Coulter Life Sciences. http://www.beckman.com/coulter-flow-cytometry/instruments/cell-sorters/moflo-astrios-eq. Accessed January 20, 2017.
28. Fox D. XDP Electronics Whitepaper Analysis of Acquisition Architectures. Beckman Coulter. http://molbiol.ru/forums/index.php?act=Attach&type=post&id=229755. Accessed January 20, 2017.
29. Lee EM, et al. Molecular methods for evaluation of virological status of nonhuman primates challenged with simian immunodeficiency or simian-human immunodeficiency viruses. *J Virol Methods*. 2010;163(2):287–294.
30. Romano JW, et al. Quantitative evaluation of simian immunodeficiency virus infection using NASBA technology. *J Virol Methods*. 2000;86(1):61–70.
31. Keele BF, et al. Identification and characterization of transmitted and early founder virus envelopes in primary HIV-1 infection. *Proc Natl Acad Sci USA*. 2008;105(21):7552–7557.
32. Shevchenko A, Tomas H, Havlis J, Olsen JV, Mann M. In-gel digestion for mass spectrometric characterization of proteins and proteomes. *Nat Protoc*. 2006;1(6):2856–2860.
33. Tamura K, Nei M. Estimation of the number of nucleotide substitutions in the control region of mitochondrial DNA in humans and chimpanzees. *Mol Biol Evol*. 1993;10(3):512–526.
34. Kumar S, Stecher G, Tamura K. MEGA7: Molecular Evolutionary Genetics Analysis Version 7.0 for Bigger Datasets. *Mol Biol Evol*. 2016;33(7):1870–1874.